Doubly excited states of the positronium molecule

Yi Zhang,[1,2] Meng-Shan Wu,[1,*] Ying Qian,[3] Kálmán Varga,[4] Hui-Li Han,[1] and Jun-Yi Zhang[1]

[1]*State Key Laboratory of Magnetic Resonance and Atomic and Molecular Physics, Innovation Academy for Precision Measurement Science and Technology, Chinese Academy of Sciences, Wuhan 430071, China*

[2]*University of Chinese Academy of Sciences, Beijing 100049, China*

[3]*School of Computer Science and Technology, East China Normal University, Shanghai 200062, China*

[4]*Department of Physics and Astronomy, Vanderbilt University, Nashville, Tennessee 37235, USA*

(Received 17 June 2020; accepted 10 July 2020; published 31 July 2020)

The projection method with explicitly correlated Gaussians is used to demonstrate the existence of two doubly excited states of the positronium molecule (Ps_2). One is below the $Ps(n = 2) + Ps(n = 2)$ threshold, with A_1 symmetry, and the other is below the $Ps(n = 2) + Ps(n = 3)$ threshold, with E symmetry. These states exist as resonances in the Ps-Ps continuum. Moreover, the resonance positions and resonance widths of the two states are calculated using the complex rotation method with basis sets obtained via the orthogonalizing pseudoprojector method. The resonance positions obtained using the complex rotation method agree with the results of the orthogonalizing pseudoprojector method. We also investigate the various structural properties of these states as well as the decay probabilities of 2γ emission due to electron-positron annihilation.

DOI: 10.1103/PhysRevA.102.012825

I. INTRODUCTION

The positronium (Ps) molecule, Ps_2, which is a special molecular system formed by two positronium atoms, has attracted much experimental and theoretical interest [1–18]. The existence of Ps_2 was first theoretically predicted by Hylleraas [1] in 1947 and was observed experimentally by Cassidy and Mills [4] in 2007. Optical spectroscopy measurements of Ps_2 for the $L = 1$ excited state were performed by the same group [5] in 2012. These experiments laid a foundation for new antiparticle phenomena, such as Ps Bose-Einstein condensation (BEC) [2] and γ-ray lasers [3].

To date, many theoretical studies have focused on this system [6–18]. Kinghorn and Poshusta [9] calculated the binding energies of the ground state and two metastable states of Ps_2 by exploiting the full permutational symmetry of the Hamiltonian, including charge-reversal symmetry. Later, Varga *et al.* [11] reported another $L = 1$ bound state with negative parity. The complete symmetry and spin problem with charge-conjugation parity was worked out by Schrader [13], and the relativistic and leading logarithmic radiative corrections of the ground and P-wave excited states were investigated by Puchalski and Czarnecki [6]. For the resonances of Ps_2, several low-lying states below the $Ps(n = 1) + Ps(n = 4)$ threshold have been predicted by Usukura and Suzuki [14] using the complex scaling method. Despite these extensive studies, however, the doubly excited states of Ps_2 have not previously been reported.

Unlike most molecules composed of normal atoms, the Ps_2 molecule can decay through the annihilation of the electron-positron pair into photons even in the ground state. This decay mode is similar to that of atomic Ps. It is well known that the annihilation of Ps depends on the overlap of the positron and electron wave functions. For this reason, the lifetime of the first excited state is longer than that of the ground state. For example, the lifetime of $Ps(1\,^1S_0)$ is 0.125 ns, while $Ps(2\,^1S_0)$ has a lifetime of 1 ns [19]. For the doubly excited states of Ps_2, the lifetime information is less well known; however, a longer lifetime is expected. It is therefore interesting to investigate the structural properties and decay probabilities of the 2γ emission of doubly excited states of Ps_2.

In this paper, we investigate the doubly excited states of Ps_2 that correspond to the $Ps(n = 2) + Ps(n \geqslant 2)$ thresholds. The structural properties of these states as well as the decay probabilities of 2γ emission due to electron-positron annihilation are also studied. The stochastic variational method (SVM) [20–23] with explicitly correlated Gaussians (ECGs) is used to describe this nonadiabatic system. To approach the doubly excited states of Ps_2, unwanted states are removed by adding the orthogonalizing pseudoprojector (OPP) operator [24,25] to the Hamiltonian. This method, the so-called projection method, can provide intrinsic information on the resonance energies of these autoionizing states of Ps_2.

This paper is organized as follows. In Sec. II, the OPP method with ECGs and the symmetry group of Ps_2 are explained. In Sec. III, the doubly excited states of the negative positronium ion (Ps^-) are calculated as a test of the OPP method. Then, the properties of two doubly excited Ps_2 states are calculated using the OPP method. The resonance positions and resonance widths of the two doubly excited Ps_2 states are also calculated using the complex rotation method in this section. A brief summary is presented in Sec. IV. Atomic units are used unless otherwise noted.

II. THEORETICAL METHOD

A. The OPP method combined with the SVM

The projection method [26,27] has been widely used for the identification of resonance states. In this method, a penalty

*mswu@wipm.ac.cn

function is added to the Hamiltonian to enforce the exclusion of certain orbitals from the active space, resulting in the autoionization of the system. This projection calculation is often called a $\hat{Q}\hat{H}\hat{Q}$ calculation. The Hamiltonian $\hat{Q}\hat{H}\hat{Q}$ is diagonalized to investigate resonant states, where $\hat{Q} = (1 - \hat{P})$ is the projection operator. For the calculation of the doubly excited states of Ps_2, the combined projection operator is defined as $\sum_{i,j}\hat{P}_{ij} = \sum_{i,j}|\phi_{1S}(\boldsymbol{r}_i - \boldsymbol{r}_j)\rangle\langle\phi_{1S}(\boldsymbol{r}_i - \boldsymbol{r}_j)|$, where $|\phi_{1S}(\boldsymbol{r}_i - \boldsymbol{r}_j)\rangle$ is the wave function of the Ps($1S$) orbital. This projection operator is slightly different from the usual definition of an atomic projection operator, and a detailed description is given below.

In the present work, the $\hat{Q}\hat{H}\hat{Q}$ Hamiltonian is approximated by adding an OPP operator to the Hamiltonian. The OPP method was first introduced by Krasnopolsky and Kukulin [28] in 1974. Mitroy and Ryzhikh [29] performed a comprehensive numerical investigation of the effects due to different strengths of the OPP operator and different sizes of basis sets. They found that the energies calculated via the OPP method will converge to those calculated by diagonalizing the $\hat{Q}\hat{H}\hat{Q}$ Hamiltonian. Compared with the $\hat{Q}\hat{H}\hat{Q}$ method, the OPP method is easier to apply. The occurrence of positron attachment to the doubly excited states of helium has been confirmed using the OPP method [25].

The modified Schrödinger equation for doubly excited Ps_2 has the following form:

$$(\hat{H} + \lambda\hat{P})\Psi = E_{\rm OPP}\Psi. \tag{1}$$

The nonrelativistic Hamiltonian $\hat{H}$ is written as

$$\hat{H} = -\sum_{i=1}^{4}\frac{\nabla^2_{\boldsymbol{r}_i}}{2} + \frac{1}{|\boldsymbol{r}_1 - \boldsymbol{r}_2|} - \frac{1}{|\boldsymbol{r}_1 - \boldsymbol{r}_3|} - \frac{1}{|\boldsymbol{r}_1 - \boldsymbol{r}_4|} - \frac{1}{|\boldsymbol{r}_2 - \boldsymbol{r}_3|} - \frac{1}{|\boldsymbol{r}_2 - \boldsymbol{r}_4|} + \frac{1}{|\boldsymbol{r}_3 - \boldsymbol{r}_4|}. \tag{2}$$

The electron coordinates are $\boldsymbol{r}_1$ and $\boldsymbol{r}_2$, while $\boldsymbol{r}_3$ and $\boldsymbol{r}_4$ denote the positron coordinates. We use r_{ij} to represent the distance between particles i and j, and its expectation value is $\langle r_{ij}\rangle = \langle\Psi|r_{ij}|\Psi\rangle$ with the OPP wave function Ψ. The expectation value of $\langle\delta_{ij}\rangle$ is also defined as $\langle\Psi|\delta(r_{ij})|\Psi\rangle$, which gives the probability of finding the two particles labeled i and j at the same point in space. The OPP operator is constructed by summing over the Ps($1S$) projection operators:

$$\lambda\hat{P} = \lambda\sum_{i,j}\hat{P}_{ij} = \lambda\sum_{i,j}|\phi_{1S}(\boldsymbol{r}_i - \boldsymbol{r}_j)\rangle\langle\phi_{1S}(\boldsymbol{r}_i - \boldsymbol{r}_j)|, \tag{3}$$

where λ is a large positive number; in the present calculations, λ is set to 10^5 a.u., which is sufficiently large compared to previous calculations [21,26–29]. The Ps($1S$) wave function $|\phi_{1S}(\boldsymbol{r}_i - \boldsymbol{r}_j)\rangle$ is expanded as a linear combination of 10 ECGs, and the obtained energy is -0.249999 a.u., where i and j are summed over all possible orbitals of electron-positron pairs. Four orbitals, namely, $|\phi_{1S}(\boldsymbol{r}_1 - \boldsymbol{r}_4)\rangle$, $|\phi_{1S}(\boldsymbol{r}_2 - \boldsymbol{r}_4)\rangle$, $|\phi_{1S}(\boldsymbol{r}_1 - \boldsymbol{r}_3)\rangle$, and $|\phi_{1S}(\boldsymbol{r}_2 - \boldsymbol{r}_3)\rangle$, are considered in the present calculations; thus, the overall calculations are complex and time consuming.

The energy $E_{\rm OPP}$ obtained using the OPP method converges to the real resonance position E_R with a small shift Δ_Q [26,30]. This relationship can be expressed as

$$E_R = E_{\rm OPP} + \Delta_Q, \tag{4}$$

where the shift Δ_Q is very small and positive in the lower S state and could originate from the original $\hat{Q}\hat{H}\hat{Q}$. Thus, the complex rotation method is needed to refine the resonance position E_R and estimate the resonance width Γ.

ECGs [22,23] are used to describe the complex Coulomb interactions between charged particles. ECGs not only describe the correlations between charged particles but also allow the matrix elements of the Hamiltonian to be evaluated easily and quickly. After the center-of-mass motion has been separated out from the Hamiltonian, the ECG basis to be used can be written as

$$\Phi_n = |\boldsymbol{\nu}|^{2K+L}\exp\left(-\frac{1}{2}\sum_{i\geqslant 1 j\geqslant 1}^{3}A^n_{ij}\boldsymbol{x}_i\cdot\boldsymbol{x}_j\right)Y_{LM}(\hat{\boldsymbol{\nu}}), \tag{5}$$

where $\boldsymbol{x}_i$ is $\boldsymbol{x}_i = \boldsymbol{r}_i - \boldsymbol{r}_4$ and $\boldsymbol{\nu} = \sum_{i=1}^{3}u_i\mathbf{x}_i$ is the global vector. The independent parameters A^n_{ij} contained in the nth symmetric matrix A^n are optimized through energy minimization using the SVM. The preexponential factor $|\boldsymbol{\nu}|^{2K+L}$ (where K is an integer and L is the total orbital angular momentum) is introduced to describe the increasing number of nodes for doubly excited states with $L = 0$ in the present calculations.

B. Permutational symmetry

The following real particle permutations of Ps_2 can be identified: the identity, 1; the interchange of the electrons, $\mathcal{P}_{12}$; the interchange of the positrons, $\mathcal{P}_{34}$; the interchange of both the positrons and the electrons, $\mathcal{P}_{12}\mathcal{P}_{34}$; the first-class charge reversals, $\mathcal{P}_{13}\mathcal{P}_{24}$ and $\mathcal{P}_{14}\mathcal{P}_{23}$; and the second-class charge reversals, $\mathcal{P}_{1324}$ and $\mathcal{P}_{1423}$. These eight permutations form a permutation group S_4, which is isomorphic to the point group D_{2d}. From knowledge of the point group D_{2d} [9,13,15], we can obtain the following symmetry projection operators $\mathcal{P}^{\mu}$ for the irreducible symmetries under particle permutations:

$$\mathcal{P}^{A_1} = \tfrac{1}{8}(1 + \mathcal{P}_{13}\mathcal{P}_{24})(1 + \mathcal{P}_{12})(1 + \mathcal{P}_{34}), \tag{6}$$

$$\mathcal{P}^{A_2} = \tfrac{1}{8}(1 - \mathcal{P}_{13}\mathcal{P}_{24})(1 + \mathcal{P}_{12})(1 + \mathcal{P}_{34}), \tag{7}$$

$$\mathcal{P}^{B_1} = \tfrac{1}{8}(1 + \mathcal{P}_{13}\mathcal{P}_{24})(1 - \mathcal{P}_{12})(1 - \mathcal{P}_{34}), \tag{8}$$

$$\mathcal{P}^{B_2} = \tfrac{1}{8}(1 - \mathcal{P}_{13}\mathcal{P}_{24})(1 - \mathcal{P}_{12})(1 - \mathcal{P}_{34}), \tag{9}$$

$$\mathcal{P}^{E_{11}} = \tfrac{1}{4}(1 - \mathcal{P}_{12}\mathcal{P}_{34} + \mathcal{P}_{13}\mathcal{P}_{24} - \mathcal{P}_{14}\mathcal{P}_{23}), \tag{10}$$

$$\mathcal{P}^{E_{12}} = \tfrac{1}{4}(\mathcal{P}_{12} - \mathcal{P}_{34} - \mathcal{P}_{1324} + \mathcal{P}_{1423}), \tag{11}$$

$$\mathcal{P}^{E_{21}} = \tfrac{1}{4}(\mathcal{P}_{12} - \mathcal{P}_{34} + \mathcal{P}_{1324} - \mathcal{P}_{1423}), \tag{12}$$

$$\mathcal{P}^{E_{22}} = \tfrac{1}{4}(1 - \mathcal{P}_{12}\mathcal{P}_{34} - \mathcal{P}_{13}\mathcal{P}_{24} + \mathcal{P}_{14}\mathcal{P}_{23}), \tag{13}$$

where $\{\mu\} = \{A_1, A_2, B_1, B_2, E_{11}, E_{12}, E_{21}, E_{22}\}$ is the set of irreducible representations of the D_{2d} group. These symmetry projectors can be applied to the wave function as one representation of the D_{2d} group. Therefore, the symmetry of

TABLE I. Resonance positions E_R, resonance widths Γ, and OPP energies $E_{\rm OPP}$ for the doubly excited $Ps^-(2s^2)$ and $Ps^-(2s3s)$ states. Comparisons with previous results are also shown. Atomic units are used.

State		$(E_R, \Gamma/2)$	$E_{\rm OPP}$
$Ps^-(2s^2)$	Present	$(-0.0760304,\ 2.154 \times 10^{-5})$	-0.0762811
	Ref. [32]	$(-0.0760304,\ 2.15 \times 10^{-5})$	
	Ref. [34]	$(-0.0760304,\ 2.15173 \times 10^{-5})$	
$Ps^-(2s3s)$	Present	$(-0.06354,\ 4.34 \times 10^{-6})$	-0.063599
	Ref. [32]	$(-0.063650,\ 5 \times 10^{-6})$	
	Ref. [34]	$(-0.063649,\ 4.33925 \times 10^{-6})$	

the wave function with L, μ, and parity π can be denoted by $L^\pi(\mu)$.

The Hamiltonian operator $\hat{H}$ that is evaluated through variational calculations usually commutes with all permutation operators. Therefore, we can formulate a convenient implementation in which all permutational operators are applied to the ket:

$$\hat{H}_{mn} = \langle \mathcal{P}^\mu \Phi_m | \hat{H} | \mathcal{P}^\mu \Phi_n \rangle = \langle \Phi_m | \hat{H} | \mathcal{P}^{\mu\dagger} \mathcal{P}^\mu \Phi_n \rangle. \quad (14)$$

In the OPP method, the projection operators do not commute with the permutation operators. The total symmetry projector $\mathcal{P}^\mu$, which actually adapts the wave function to one representation of the D_{2d} group, should be applied to both the bra and the ket:

$$\hat{H}_{mn} + \lambda \hat{P}_{mn} = \langle \mathcal{P}^\mu \Phi_m | \hat{H} + \lambda \hat{P} | \mathcal{P}^\mu \Phi_n \rangle, \quad (15)$$

which makes convergence rather slow. Meanwhile, the calculation of $\hat{H} + \lambda \hat{P}$ can result in the problem of linear dependence much more easily than in the case of $\hat{H}$. For this reason, the variational calculation becomes numerically unstable with further enlargement of the ECG basis.

C. Complex rotation method

The resonance positions and resonance widths of these autoionizing states can be calculated using the complex rotation (CR) method [31]. In the CR method, the transformation $r \to \exp(i\theta) r$ is carried out to make the resonant wave function square integrable and amenable to basis-set expansion. With the application of this rotation, the Hamiltonian with Coulombic interactions becomes

$$H_\theta = \exp(-2i\theta) T + \exp(-i\theta) V. \quad (16)$$

The resonance position E_R and resonance width Γ are determined by solving the complex eigenvalue problem. The complex eigenvalue is defined as $E^c = E_R - i\Gamma/2$. The resonant states can be identified by adjusting the rotation parameter θ, and their energies show relatively little change as θ varies, which means that $\partial |E^c| / \partial\theta$ becomes a minimum. To locate the resonant states more accurately, we introduce dilation parameters $\alpha = 0.99$, 1, and 1.01. Here, dilation is defined as the following transformation of all coordinates of the dynamical system: $r \to r\alpha$. Different dilation parameters will relate to the same resonant states.

III. RESULTS AND DISCUSSION

In this paper, we mainly focus on the calculation of the properties of doubly excited Ps_2 states under A_1 and E symmetry. We have also performed OPP calculations for the doubly excited Ps_2 state under B_1 symmetry. A basis with 5000 dimensions was used to obtain the energy $E_{\rm OPP} = -0.12495$ a.u., which is higher than the threshold energy $E_{\rm Ps(2S)+Ps(2S)} = -0.125$ a.u. For B_2 and A_2 symmetry, the corresponding threshold is $Ps(2S) + Ps(3P)$, which means that not only the $Ps(1S)$ orbital but also the $Ps(2P)$ orbital need to be excluded in the OPP calculations. Such OPP calculations require large-scale computational resources and are beyond our current computing capabilities.

A. Example calculation using the OPP method for Ps^-

Extensive calculations have been performed for the doubly excited Ps^- states using the CR method [32–34]. In this section, calculations for the doubly excited $Ps^-(2s^2)$ and $Ps^-(2s3s)$ states are carried out to validate the OPP method. First, the OPP method combined with the SVM is used to obtain the OPP energies and wave functions for these two doubly excited states. Then, the CR method is used to refine the resonance positions (E_R) and widths (Γ) using the basis sets obtained via the OPP method.

The present results for the doubly excited $Ps^-(2s^2)$ and $Ps^-(2s3s)$ states and comparisons with previous results [32,34] are given in Table I. In the present OPP calculations, the wave functions are expanded with 500 ECGs. We can see that the values of $E_{\rm OPP}$ are very close to the E_R values, with small discrepancies of $|\Delta_Q/E_R| = 0.33\%$ and 0.09% for $Ps^-(2s^2)$ and $Ps^-(2s3s)$, respectively. Theoretically, the values of Δ_Q could be reduced through further optimization or enlargement of the ECG basis. However, the calculations will become numerically unstable due to the linear dependence problem. Table I also shows that the present values of the resonance positions and widths are in good agreement with those of Ho [32] and Li and Shakeshaft [34]. This means that the basis sets we obtain using the OPP method (OPP basis sets) are of high quality and are suitable for CR calculations.

B. Doubly excited Ps_2 state with A_1 symmetry

The doubly excited Ps_2 state with A_1 symmetry can be denoted by $0^+(A_1)$. The symmetry projector applied to the spatial part of the basis functions is $\mathcal{P}^{A_1} = (1 + P_{13}P_{24})(1 + P_{12})(1 + P_{34})$; see Eq. (6). The spins of the electrons and positrons in $0^+(A_1)$ are equal to zero, i.e., $S^- = 0$ and $S^+ = 0$.

TABLE II. Expectation values of various structural properties for the doubly excited Ps_2 state with A_1 symmetry. N is the dimensionality of the basis. For convenience, we use $\langle R_1\rangle = \langle r_{14}\rangle = \langle r_{24}\rangle = \langle r_{13}\rangle = \langle r_{23}\rangle$ and $\langle R_2\rangle = \langle r_{12}\rangle = \langle r_{34}\rangle$ to represent the expectation values of the electron-positron distance and the electron-electron (or positron-positron) distance, respectively. In addition, $\langle\Delta_1\rangle = \langle\delta_{14}\rangle = \langle\delta_{24}\rangle = \langle\delta_{13}\rangle = \langle\delta_{23}\rangle$ and $\langle\Delta_2\rangle = \langle\delta_{12}\rangle = \langle\delta_{34}\rangle$ represent the probability of finding an electron and a positron at the same point in space and the probability of finding two electrons (or two positrons) at the same point in space, respectively. Atomic units are used.

N	Energy	$\langle R_1\rangle$	$\langle R_2\rangle$	$\langle R_1^2\rangle$	$\langle R_2^2\rangle$	$10^4\langle\Delta_1\rangle$	$10^7\langle\Delta_2\rangle$
3000	−0.12531	19.83	29.72	641.1	1185	6.725	7.440
3500	−0.12540	20.33	30.74	700.0	1330	6.462	6.696
4000	−0.12544	20.68	31.44	745.5	1394	6.330	6.336
4500	−0.12548	20.93	31.95	782.3	1467	6.259	6.116
5000	−0.12550	21.11	32.31	809.9	1522	6.210	5.919

The results of convergence tests for the OPP energy and other structural properties of this state as functions of the dimensionality N of the basis are reported in Table II. In this table, we use $\langle R_1\rangle = \langle r_{14}\rangle = \langle r_{24}\rangle = \langle r_{13}\rangle = \langle r_{23}\rangle$ to represent the expectation value of the distance between an electron and a positron and $\langle R_2\rangle = \langle r_{12}\rangle = \langle r_{34}\rangle$ to represent the expectation value of the distance between the two electrons (or the two positrons). For convenience, we also define $\langle\Delta_1\rangle = \langle\delta_{14}\rangle = \langle\delta_{24}\rangle = \langle\delta_{13}\rangle = \langle\delta_{23}\rangle$ to represent the probability of finding an electron and a positron at the same point in space and $\langle\Delta_2\rangle = \langle\delta_{12}\rangle = \langle\delta_{34}\rangle$ to represent the probability of finding two electrons (or two positrons) at the same point in space in Table II.

From Table II, we can see that the energy converges to 10^{-4} a.u. and that the expectation values converge to two significant figures with the largest basis set ($N = 5000$). The basis sets used in the present calculations are very large compared with that used for the calculation of the ground-state properties of Ps_2, which requires only a basis with $N = 200$ dimensions to make the energy converge to at least 10^{-6} a.u.

Table II shows that the calculated $0^+(A_1)$ energy $E_{\rm OPP} = -0.12550$ a.u. is lower than the relevant threshold energy $E_{\rm Ps(2S)+Ps(2S)} = -0.125$ a.u. by only 4%, and the expectation value of $\langle R_2\rangle$ is larger than that of $\langle R_1\rangle$. On the other hand, the expectation values of $\langle\delta_{ij}\rangle$ also consistently show that the value of $\langle\Delta_1\rangle$ is larger than that of $\langle\Delta_2\rangle$. All of these results indicate that the structure of this doubly excited state could be dominated by a [Ps(2S) + Ps(2S)]-like configuration.

Compared to the average interparticle distances, the probability density distributions of the interparticle distances provide more information about the structure of this doubly excited state. We can define the probability density distribution of the distance between particles i and j as

$$\rho(r_{ij}) = \int d\Omega_{\mathbf{r}_{ij}} \langle\Psi|\delta\left(\sum_{k=1}^{3} c_k\mathbf{x}_k - \mathbf{r}_{ij}\right)|\Psi\rangle r_{ij}^2, \qquad (17)$$

where $\langle\cdots\rangle$ denotes the integration over the relative coordinates ($\mathbf{x}_1$, $\mathbf{x}_2$, and $\mathbf{x}_3$) and $\int d\Omega_{\mathbf{r}_{ij}}$ denotes the integration over the angle of $\mathbf{r}_{ij}$. $\rho(r_{ij})$ can be easily obtained since the matrix elements for the Dirac delta function δ can be analytically calculated using the ECG basis. The probability density distributions of R_1 and R_2 for this doubly excited state are shown in Fig. 1. We can see that $\rho(R_1)$ has a peak near 12 a.u. and a narrow plateau near 2 a.u. Since the radial probability density distribution of Ps(2S) has two peaks, this structure of $\rho(R_1)$ could originate from a [Ps(2S)-Ps(2S)]-like configuration. The figure also shows that $\rho(R_2)$ has only one peak, which is near 20 a.u.

The special decay mode in which electron-positron pair annihilation leads to photon emission plays an important role in the experimental observation of Ps_2. Electron-positron pair annihilation in the Ps_2 system results in the emission of either two photons (2γ annihilation) or more photons ($n\gamma$ annihilation). The main process here is 2γ annihilation, and the corresponding annihilation rate $\Gamma_{2\gamma}$ for this doubly excited state can be written as [23,35]

$$\Gamma_{2\gamma} = 4\pi\alpha^3\langle\delta(r_{14})\rangle = 1/\tau, \qquad (18)$$

where τ is the corresponding lifetime. With the value of $\langle\Delta_1\rangle$ given in Table II, the value of $\Gamma_{2\gamma}$ is $\Gamma_{2\gamma} = 1/(7.9\,\text{ns})$ for the $0^+(A_1)$ state. Compared with the lifetime of the ground state of Ps_2 with A_1 symmetry, $\tau = 0.22455(6)$ ns [6], the lifetime of this doubly excited state is much longer.

The OPP energy $E_{\rm OPP}$ can be regarded as a good approximation of the resonance position E_R, whereas the resonance width Γ cannot be obtained directly through the OPP calculation. With the OPP basis sets for this doubly excited state,

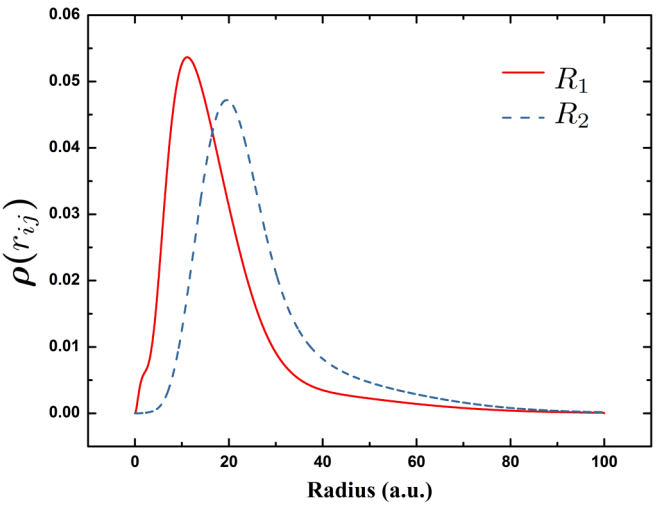

FIG. 1. The probability density distributions of R_1 and R_2 for the doubly excited Ps_2 state with A_1 symmetry. $R_1 = r_{14} = r_{24} = r_{13} = r_{23}$ represents the distance between an electron and a positron. $R_2 = r_{12} = r_{34}$ represents the distance between the two electrons (or the two positrons). Atomic units are used.

TABLE III. Comparison between the OPP energies and resonance parameters for the doubly excited Ps_2 states with A_1 and E symmetry.

State	E_{OPP}	E_R	$\Gamma/2$
A_1	−0.12550	−0.12522	0.0000461
E	−0.099298	−0.09672	0.000634

the CR method can be used to calculate E_R and Γ. To better represent the wave functions of the breakup channels, outer basis functions [24,36,37] are added to the OPP basis set. Only the $Ps(2S) + Ps(2S)$ breakup channel is considered in the present CR calculation, and the $Ps(2S) + Ps(2S)$ outer basis functions are written as

$$\Phi_n^{\text{out}} = \exp(-\alpha_n R^2)\phi_{Ps(2s)}(\mathbf{r}_1 - \mathbf{r}_3)\phi_{Ps(2s)}(\mathbf{r}_2 - \mathbf{r}_4). \quad (19)$$

Here, $\exp(-\alpha_n R^2)$ is called the connected function, and R is the relative distance between the two $Ps(2s)$ atoms. The $Ps(2S)$ wave function $\phi_{Ps(2s)}$ is expanded as a linear combination of 12 ECGs (which yields an energy of −0.0624999 a.u.). In the present CR calculation for this doubly excited Ps_2 state $0^+(A_1)$, six outer basis functions are added (further enlargement of Φ_n^{out} will result in the linear dependence problem). The exponents α_n are defined as $\alpha_n = 0.01/2.5^n$. Thus, the final basis for the CR calculation consists of 5006 ECGs, including 5000 OPP ECGs and 6 Φ_n^{out} ECGs.

The complex trajectories for this doubly excited state are shown in Fig. 2. Using the dilation transformation, three complex trajectories with different dilation parameters $\alpha =$ 0.99, 1, and 1.01 are plotted in this figure. We can see that with these three dilations, the resonance remains located at the same position, resulting in the resonance parameters $E_R =$ −0.12522 a.u. and $\Gamma/2 = 0.000461$ a.u.

The OPP energies and the resonance parameters are listed for comparison in Table III. We can see that the OPP energy E_{OPP} is in good agreement with the E_R value given by the CR calculation, with a discrepancy of $|\Delta_Q/E_R| = 0.22\%$, for the $0^+(A_1)$ state.

C. Doubly excited Ps_2 state with E symmetry

The total symmetry projector $\mathcal{P}^{E_{11}} = 1 - P_{12}P_{34} + P_{13}P_{24} - P_{14}P_{23}$ is chosen to represent E symmetry with positive parity. In contrast to A_1 symmetry, E symmetry is not associated with a unique set of spins. The spins of the electrons and positrons for E symmetry can be a mixture of $(S^- = 0, S^+ = 1)$ and $(S^- = 1, S^+ = 0)$. Thus, the expectation value $\langle O_{14}\rangle$ is not equal to $\langle O_{24}\rangle$, where $\hat{O}$ stands for an arbitrary operator. This can be clearly seen in Table IV, where $\langle r_{14}\rangle \neq \langle r_{24}\rangle$ and $\langle \delta_{14}\rangle \neq \langle \delta_{24}\rangle$. Table IV shows the results of convergence tests for the OPP energy and other structural properties of this state as functions of the basis dimensionality N. We define $\langle R_1\rangle = \langle r_{14}\rangle = \langle r_{23}\rangle$ and $\langle R_2\rangle = \langle r_{13}\rangle = \langle r_{24}\rangle$ to represent the two different expectation values of the distances between an electron and a positron. $\langle R_3\rangle = \langle r_{12}\rangle = \langle r_{34}\rangle$ represents the expectation value of the distance between the two electrons (or the two positrons). $\langle \Delta_1\rangle = \langle \delta_{14}\rangle = \langle \delta_{23}\rangle$ and $\langle \Delta_2\rangle = \langle \delta_{13}\rangle = \langle \delta_{24}\rangle$ represent the probabilities of finding an electron and a positron at the same point in space. Meanwhile, for simplicity, $\langle \Delta_3\rangle = \langle \delta_{12}\rangle = \langle \delta_{34}\rangle$ is also defined to represent the probability of finding two electrons (or two positrons) at the same point in space in Table IV.

For E symmetry, the energy converges to 10^{-4} a.u., and the expectation values converge to two significant figures with the largest basis set ($N = 5000$). The OPP energy of this doubly

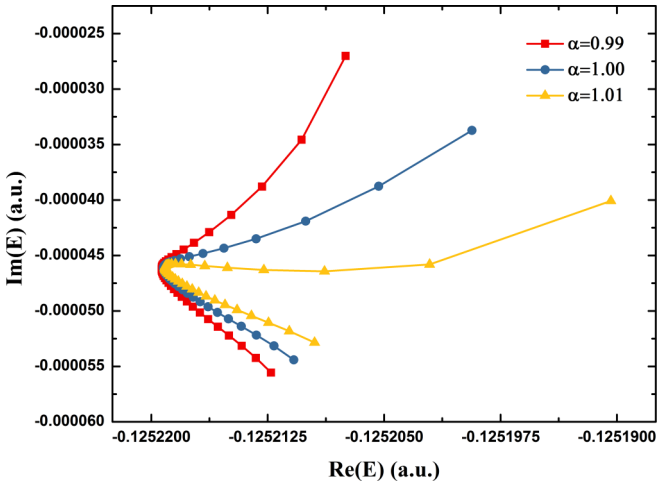

FIG. 2. CR diagram for the doubly excited Ps_2 state with A_1 symmetry. α is the parameter of the dilation transformation.

TABLE IV. Expectation values of various structural properties for the doubly excited Ps_2 state with E symmetry. N is the dimensionality of the basis. For convenience, $\langle R_1\rangle = \langle r_{14}\rangle = \langle r_{23}\rangle$ and $\langle R_2\rangle = \langle r_{13}\rangle = \langle r_{24}\rangle$ represent the expectation values of the electron-positron distances, and $\langle R_3\rangle = \langle r_{12}\rangle = \langle r_{34}\rangle$ represents the expected distance between the two electrons (or the two positrons). In addition, $\langle \Delta_1\rangle = \langle \delta_{14}\rangle = \langle \delta_{23}\rangle$ and $\langle \Delta_2\rangle = \langle \delta_{13}\rangle = \langle \delta_{24}\rangle$ represent the probabilities of finding an electron and a positron at the same point in space, and $\langle \Delta_3\rangle = \langle \delta_{12}\rangle = \langle \delta_{34}\rangle$ represents the probability of finding two electrons (or two positrons) at the same point in space. Atomic units are used.

N	Energy	$\langle R_1\rangle$	$\langle R_2\rangle$	$\langle R_3\rangle$	$\langle R_1^2\rangle$	$\langle R_2^2\rangle$	$\langle R_3^2\rangle$	$10^3\langle \Delta_1\rangle$	$10^4\langle \Delta_2\rangle$	$10^7\langle \Delta_3\rangle$
3000	−0.099227	18.06	31.60	32.52	396.3	1219	1180	1.598	3.391	1.381
3500	−0.099243	18.08	31.61	32.55	398.1	1220	1183	1.611	3.520	1.331
4000	−0.099269	18.12	31.62	32.58	401.5	1224	1187	1.606	3.537	1.310
4500	−0.099287	18.17	31.60	32.58	404.2	1223	1189	1.603	3.549	1.280
5000	−0.099298	18.19	31.59	32.59	406.7	1222	1190	1.602	3.553	1.271

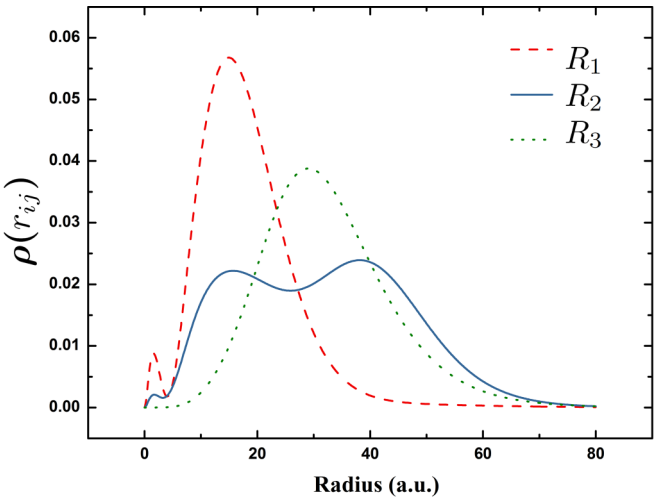

FIG. 3. The probability density distributions of R_1, R_2, and R_3 for the doubly excited Ps_2 state with E symmetry. $R_1 = r_{14} = r_{23}$ and $R_2 = r_{13} = r_{24}$ represent the distances between an electron and a positron. $R_3 = r_{12} = r_{34}$ represents the distance between the two electrons (or the two positrons). Atomic units are used.

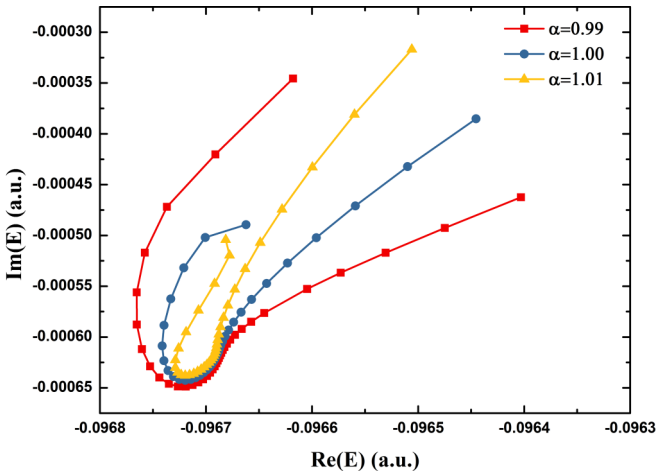

FIG. 4. CR diagram for the doubly excited Ps_2 state with E symmetry. α is the parameter of the dilation transformation.

excited state, $E_{\rm OPP} = -0.099298$ a.u., is much lower than the relevant threshold energy, $E_{\rm Ps(2S)+Ps(3S)} = -0.0902778$ a.u.

Since the value of $\langle\Delta_1\rangle$ is different from that of $\langle\Delta_2\rangle$ in the case of E symmetry, it is necessary to modify the 2γ annihilation rate expression given in Eq. (18) as follows:

$$\Gamma_{2\gamma} = 2\pi\alpha^3\langle\delta(r_{14})\rangle + 2\pi\alpha^3\langle\delta(r_{24})\rangle = 1/\tau. \qquad (20)$$

Using Eq. (20) and the values of $\langle\Delta_1\rangle$ and $\langle\Delta_2\rangle$ in Table IV, we find that $\Gamma_{2\gamma} = 1/(5.1\,\text{ns})$. Thus, the lifetime of this doubly excited state is longer than that of the ground state of Ps_2 with E symmetry ($\tau = 0.44$ ns) [12].

The probability density distributions of R_1, R_2, and R_3 for this doubly excited state are shown in Fig. 3. We can see that $\rho(R_1)$ has two peaks, which are located near 1.5 and 15 a.u. These two peaks should originate from the Ps($2S$) configuration. Meanwhile, $\rho(R_2)$ has three peaks, near 1.5, 15, and 38 a.u., which should originate from Ps($3S$). $\rho(R_3)$ has only one peak, near 29 a.u. From the probability density distributions and the OPP energy, we can infer that the structure of this doubly excited state could be dominated by a [Ps($2S$)-Ps($3S$)]-like configuration.

Similarly, the CR calculation is also carried out for this doubly excited state. Only the Ps($2S$) + Ps($3S$) breakup channel is considered in the present CR calculation for this state, and the corresponding outer basis functions are written as

$$\Phi_n^{\rm out} = \exp(-\alpha_n R^2)\phi_{Ps\rm Ps}(\mathbf{r}_1 - \mathbf{r}_3)\phi_{Ps\rm Ps}(\mathbf{r}_2 - \mathbf{r}_4). \qquad (21)$$

The Ps($2S$) wave function $\phi_{\rm Ps(2s)}$ is expressed as given above, while the Ps($3S$) wave function $\phi_{\rm Ps(3s)}$ is expanded as a linear combination of 16 ECGs (the energy of this state is -0.0277777 a.u.). In the final calculation, six outer basis functions are added to the 5000 OPP ECGs. The exponents α_n are defined as $\alpha_n = 0.01/3^n$. Three complex trajectories with the dilation parameters $\alpha = 0.99$, 1, and 1.01 are plotted in Fig. 4. We can see that the resonance position is located at $\theta = 0.20$ rad, and the resonance parameters are $E_R = -0.09675$ a.u. and $\Gamma/2 = 0.000634$ a.u. The OPP energy $E_{\rm OPP}$ of this state also provides a good approximation of E_R, with a discrepancy of $|\Delta_Q/E_R| = 2.7\%$.

IV. CONCLUSION

The doubly excited $0^+(A_1)$ and $0^+(E)$ states of Ps_2 have been confirmed using the projection method with explicitly correlated Gaussians. The energies and relevant thresholds are shown in Fig. 5. The energy of the $0^+(A_1)$ state is -0.12550 a.u., which is related to the Ps($2S$) + Ps($2S$) threshold, while the $0^+(E)$ state has an energy of -0.099298 a.u., which is related to the Ps($2S$) + Ps($3S$) threshold. Moreover, the resonance positions and resonance widths of the two states are calculated using the CR method with the OPP basis sets. The OPP energies $E_{\rm OPP}$ are in good agreement with the resonance positions E_R obtained using the CR method, showing the high quality of the OPP basis sets. Various structural properties of the two states as well as the decay probabilities

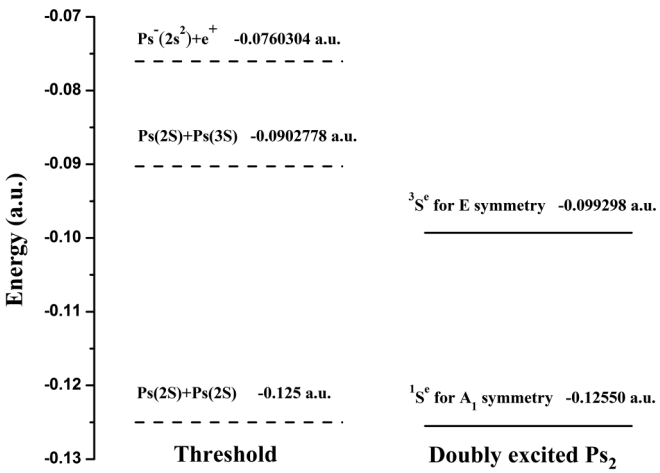

FIG. 5. The energy spectrum of the two doubly excited Ps_2 states. The two-body decay thresholds are shown as dotted lines.

of 2γ emission due to electron-positron annihilation are also studied. We find that the lifetime of the doubly excited state with A_1 symmetry is 7.9 ns, which is much longer than the lifetime of the ground state with the same symmetry. For E symmetry, the lifetime of the corresponding doubly excited state is 5.1 ns, which is also longer than that of the ground state of Ps_2 with the same symmetry. These doubly excited states of Ps_2 have not previously been reported. The identification of these autoionizing states of Ps_2 could present a new approach for future spectroscopic measurements of Ps complexes.

ACKNOWLEDGMENTS

We thank Ting-Yun Shi for useful discussions and suggestions. This work was supported by the National Natural Science Foundation of China under Grants No. 11704399, No. 11874391, and No. 11934014, by the Strategic Priority Research Program of the Chinese Academy of Sciences under Grant No. XDB21030300, and by the National Key Research and Development Program of China under Grant No. 2017YFA0304402.

[1] E. A. Hylleraas, Phys. Rev. **71**, 491 (1947).
[2] P. M. Platzman and A. P. Mills, Phys. Rev. B **49**, 454 (1994).
[3] G. C. Baldwin, J. C. Solem, and V. I. Gol'danskii, Rev. Mod. Phys. **53**, 687 (1981).
[4] D. B. Cassidy and A. P. Mills, Jr., Nature (London) **449**, 195 (2007).
[5] D. B. Cassidy, T. H. Hisakado, H. W. K. Tom, and A. P. Mills, Phys. Rev. Lett. **108**, 133402 (2012).
[6] M. Puchalski and A. Czarnecki, Phys. Rev. Lett. **101**, 183001 (2008).
[7] Y. K. Ho, Phys. Rev. A **33**, 3584 (1986).
[8] Y. K. Ho, Phys. Rev. A **39**, 2709 (1989).
[9] D. B. Kinghorn and R. D. Poshusta, Phys. Rev. A **47**, 3671 (1993).
[10] P. M. Kozlowski and L. Adamowicz, Phys. Rev. A **48**, 1903 (1993).
[11] K. Varga, J. Usukura, and Y. Suzuki, Phys. Rev. Lett. **80**, 1876 (1998).
[12] Y. Suzuki and J. Usukura, Nucl. Instrum. Methods Phys. Res., Sect. B **171**, 67 (2000).
[13] D. M. Schrader, Phys. Rev. Lett. **92**, 043401 (2004).
[14] J. Usukura and Y. Suzuki, Phys. Rev. A **66**, 010502(R) (2002).
[15] C. G. Bao and T. Y. Shi, Phys. Rev. A **67**, 042505 (2003).
[16] T. K. Rebane, V. S. Zotev, and O. N. Yhsupov, Zh. Eksp. Teor. Fiz. **110**, 55 (1996).
[17] P. M. Kozlowski and L. Adamowicz, J. Phys. Chem. **100**, 6266 (1996).
[18] S. K. Adhikari, Phys. Lett. A **294**, 308 (2002).
[19] P. A. M. Dirac, Math. Proc. Cambridge Philos. Soc. **26**, 361 (1930).
[20] K. Varga and Y. Suzuki, Phys. Rev. C **52**, 2885 (1995).
[21] G. G. Ryzhikh, J. Mitroy, and K. Varga, J. Phys. B **31**, 3965 (1998).
[22] J. Mitroy, S. Bubin, W. Horiuchi, Y. Suzuki, L. Adamowicz, W. Cencek, K. Szalewicz, J. Komasa, D. Blume, and K. Varga, Rev. Mod. Phys. **85**, 693 (2013).
[23] Y. Suzuki, M. Suzuki, and K. Varga, *Stochastic Variational Approach to Quantum-Mechanical Few-Body Problems*, Vol. 54 (Springer, Berlin, 1998).
[24] J. Mitroy and J. Grineviciute, Phys. Rev. A **88**, 022710 (2013).
[25] M. W. J. Bromley, J. Mitroy, and K. Varga, Phys. Rev. Lett. **109**, 063201 (2012).
[26] A. K. Bhatia, A. Temkin, and J. F. Perkins, Phys. Rev. **153**, 177 (1967).
[27] A. K. Bhatia and A. Temkin, Phys. Rev. A **11**, 2018 (1975).
[28] V. M. Krasnopolskij and V. I. Kukulin, Yad. Fiz. **20**, 883 (1974).
[29] J. Mitroy and G. Ryzhikh, Comput. Phys. Commun. **123**, 103 (1999).
[30] T. F. O'Malley and S. Geltman, Phys. Rev. **137**, A1344 (1965).
[31] Y. Ho, Phys. Rep. **99**, 1 (1983).
[32] Y. Ho, Phys. Lett. A **102**, 348 (1984).
[33] Z. Papp, J. Darai, C.-Y. Hu, Z. T. Hlousek, B. Kónya, and S. L. Yakovlev, Phys. Rev. A **65**, 032725 (2002).
[34] T. Li and R. Shakeshaft, Phys. Rev. A **71**, 052505 (2005).
[35] A. M. Frolov, S. I. Kryuchkov, and V. H. Smith, Phys. Rev. A **51**, 4514 (1995).
[36] I. A. Ivanov, J. Mitroy, and K. Varga, Phys. Rev. Lett. **87**, 063201 (2001).
[37] I. A. Ivanov, J. Mitroy, and K. Varga, Phys. Rev. A **65**, 032703 (2002).